WWLLN Energetic Lightning Events are Different from Optical Superbolts

Michael Peterson[1]

[1] ISR-2, Los Alamos National Laboratory, Los Alamos, New Mexico

Corresponding author: Michael Peterson (mpeterson@lanl.gov)

Key Points:

- Optical and WWLLN VLF energies are compared in superbolt and high WWLLN energy cases
- Optical superbolts are associated with large megaflashes typically found in stratiform clouds and do not reach the WWLLN 1 MJ threshold
- WWLLN high energy events do not produce strong optical flashes, and arise in convective thunderstorm cores with low flash rates

LA-UR-23-23538

Abstract

The most powerful optical emissions from lightning have been described as "superbolts" since the 1970s. In 2019, Holzworth et al. (2019) applied the superbolt label to the most energetic Radio Frequency (RF) emissions measured by the World Wide Lightning Location Network (WWLLN). In this study, we compare the WWLLN energies to optical measurements by the photodiode detector (PDD) on the Fast On-orbit Recording of Transient Events (FORTE) satellite and the Geostationary Lightning Mappers (GLMs) on NOAA's Geostationary Operational Environmental Satellites (GOES) to assess whether WWLLN high energy events coincide with optical superbolts. We find no overlap between traditional superbolts and WWLLN high energy events. Optical superbolts are not energetic to WWLLN, while WWLLN superbolts are not optically bright. Additionally, the top WWLLN sources occur in a different meteorological context than superbolts. Despite some similarities in their overall global patterns of occurrence, WWLLN high energy events correspond to a different phenomenon.

Plain Language Summary

Where do the most powerful lightning signals on Earth come from? The answer depends on the wavelength of radiation being measured. We typically use the flashes of optical light produced by lightning to make that assessment. These top cases are known as "superbolts" and typically arise from long-horizontal discharges that we call "megaflashes," which are very effective light sources. A recent study by Holzworth et al. (2019) used radio waves in the Very Low Frequency (VLF) band recorded by the World Wide Lightning Location Network (WWLLN) to assess lightning intensity. While they call their most energetic events superbolts, our comparisons with optical sensors show that they are a distinct phenomenon. WWLLN high energy events come from small flashes in the thunderstorm core rather than megaflashes outside of convection. We hypothesize factors that give rise to WWLLN high energy events, which need to be investigated in future work.

1 Introduction

In the heart of the Cold War, Turman (1977) published lightning observations from the United States' Vela satellite constellation in the scientific literature. The lightning reported by Turman (1977) was not the standard collection of flashes that would later be observed by optical satellite-based sensors to construct the space-based lightning climatologies (Christian et al., 2003, Albrecht et al., 2016, Peterson et al., 2021) used in physical research today. Instead, Turman (1977) focused on the most powerful optical emissions generated by lightning – which he termed "superbolts."

Turman (1977) found that superbolts had peak optical powers two orders of magnitude greater than ordinary lightning – radiating an estimated 10^{11} – 10^{12} W at the source with total energies integrated over the pulse exceeding 10^{8} J. Turman (1977) also noted that superbolts have a distinct pattern of occurrence that differs from normal lightning. 9-in-10 lightning flashes are produced by convective thunderstorms (Peterson and Liu, 2011) that arise as a consequence of atmospheric instability and local lifting mechanisms in regions with adequate moisture. For this reason, there are global lightning "hotspots" (Albrecht et al., 2016) in locations on the Earth where favorable conditions are frequently met. These so-called lightning "chimneys" are found

in the tropics, and include Lake Maracaibo in South America, the Congo Basin in Africa, and the Maritime Continent in Asia (Whipple and Scrase, 1936; references in Williams, 2005).

In contrast to ordinary lightning, Turman's superbolts occur in environments that are unfavorable for lightning production: mid-latitude cold-season storms with a notable hotspot in the seas surrounding near Japan. This distinction implies that superbolts are not merely the tip of the optical power spectrum from normal lightning, but rather a rare class of discharge enabled by the unique environment in which they form. Turman (1977) and subsequent comments speculated on the origins of these events, but investigations were limited by the available measurements of the era.

Advances in lightning detection since Turman's 1977 study are allowing us to clarify the origins of this extreme yet incredibly rare lightning. In 1997, the Fast On-orbit Recording of Transient Events (FORTE: Light, 2020) satellite was launched that included a photodiode detector (PDD: Kirkland et al., 2001) capable of identifying the superbolts described by Turman (1977). The Low Earth Orbit (LEO) of FORTE limited its observations to minute-scale thunderstorm snapshots, making it unlikely for a superbolt to occur within the PDD Field of View (FOV) while the satellite was overhead. Over a period of 12 years in orbit, FORTE found itself in the right place at the right time to observe tens of thousands of 10^{11} W events, and dozens of terawatt-class superbolts. Ground-based lightning detection networks were also improving and becoming more ubiquitous during the FORTE mission. We used observations by the National Lightning Detection Network (NLDN: Cummins and Murphy, 2009) to confirm that the more powerful superbolts (> 350 MW) over the United States were commonly produced by high peak current positive Cloud-to-Ground (CG) lightning strokes (Peterson and Kirkland, 2020).

Our subsequent analyses with NOAA's Geostationary Lightning Mappers (GLMs: Rudlosky et al., 2019) – optical lightning detectors on the Geostationary Operational Environmental Satellites (GOES) – also linked the most energetic superbolts to long-horizontal lightning "megaflashes" that propagate through expansive electrified clouds outside of the convective thunderstorm core (Peterson and Lay, 2020). We hypothesize that superbolts arise as a consequence of these extensive networks of lightning channels that are efficient at mobilizing vast quantities of charge from across a large reservoir while serving as extended optical sources (rather than the typical point sources) whose individual channel segments all contribute to the total optical output.

Towards the end of the FORTE PDD record (April 2009 and onward), the World Wide Lightning Location Network (WWLLN) began saving the required station data to compute the far-radiated Very Low Frequency (VLF)-band Radio Frequency (RF) energies from lightning strokes. This radiation propagates in the Earth-ionosphere waveguide with low attenuation over distances up to thousands of kilometers from the source to WWLLN receivers distributed across the globe. Attenuation is corrected using the U.S. Navy's Long Wavelength Propagation Capability code (see Thomson, 2010) to estimate the energy of the source in the 5-18 kHz band.

Holzworth et al. (2019) used these WWLLN energies to identify the top emitters in the VLF band and labeled these lightning events "superbolts." Their justification for making this assessment based on VLF energy, alone, was that some of the top WWLLN strokes showed a similar pattern of occurrence to the Vela and FORTE superbolt distributions – including a

wintertime mid-latitude maximum. They did not correlate WWLLN VLF energies with optical outputs or offer a hypothesis for the cause of extreme WWLLN events.

We must be careful with any assumption that extreme RF output implies exceptional optical output because the two phenomenologies are sensitive to different aspects of the lightning discharge. Optical emissions that escape to space are created by the extreme heating of the lightning channels in the clouds, where the atmospheric constituent gasses go through dissociation, excitation, and recombination to produce particularly strong signals in certain spectral bands (the 777.4 nm band used by GLM is an Oxygen line triplet). These signals are then attenuated by absorption and scattering in the clouds, which reduces the contributions from low altitudes (Thomas et al., 2000).

RF emissions, meanwhile, are generated by the movement of charge through the lightning channels. WWLLN's VLF receivers are particularly sensitive to large transient currents (Cummins and Murphy, 2009), while factors that are important for optical emission (i.e., cloud scattering, horizontal channel dimensions) are not important for WWLLN. The extensive comparisons between optical and VHF-band RF emissions in the literature demonstrate why conflating RF and optical outputs may not be appropriate. The most powerful natural emitters of VHF radiation are Compact Intracloud Discharges (CIDs) – lightning events within thunderclouds that are inferred to have short (< 1 km) channel lengths dominated by cold streamers rather than hot leaders. As a result, the top VHF events at the tip of the lightning power spectrum produce little, if any, optical emissions in the common spectral bands for lightning detection (Light and Jacobson, 2002). While perhaps not to the extreme extent of VHF, there may still be a disconnect between VLF and optical lightning outputs.

Assessing whether the most energetic WWLLN events correspond to optical superbolts requires direct comparisons between the optical and VLF outputs from lightning events. In this study, we identify WWLLN strokes jointly detected by either the FORTE PDD or GLM, and compare the emissions between each phenomenology.

2 Data and Methods

2.1 The World Wide Lightning Location Network (WWLLN)

WWLLN consists of ~80 VLF sensors across the globe that detect atmospheric electromagnetic impulses generated by lightning. Waveforms within a band extending from 100 Hz to 24 kHz are recorded at each station and used to determine the Time of Group Arrival (TOGA) of the incident radiation (Dowden et al., 2002) with an accuracy of ~1 μs. The energies reported by WWLLN are derived from this station data, using a 5-18 kHz sub-band within the broadband signal. The TOGAs from each station in the network are compared to identify joint detections of the same lightning stroke. Whenever five or more WWLLN stations detect a stroke, their locations and arrival times are used to compute the location of the stroke on the Earth. Generally, WWLLN stroke locations are considered accurate to within ~10 km (Abarca et al., 2010).

Holzworth et al. (2019) identifies high energy events as WWLLN strokes with (1) reported energies > 1 MJ, (2) 7-or-more reporting stations, and (3) the standard error of the

energy fit < 30% of the reported stroke energy. However, not every reporting station will provide an energy measurement. In extreme cases, a 7-station event might include only 1 or 2 energy measurements. Our analyses of the WWLLN events indicate that Holzworth et al. (2019) further remove events with only one station providing an energy measurement. We will use the same filtering in this study, but we will consider WWLLN data from April 2009 through 2022.

2.2 The FORTE Photodiode Detector (PDD)

The PDD was a silicon photodiode detector that recorded broadband (0.4–1.1 μm) optical waveforms produced by transient events across its 80° circular Field of View (FOV) below the FORTE satellite. It had a sampling interval of 15 μs and was usually operated in its self-triggering mode where it reported 1.9 ms of data in each record. The PDD had three known issues that impact its ability to detect superbolts.

First, each event was followed by a period of dead time that was comparable to the record length. If the PDD triggers on the initial activity within the cloud before a CG, for example, any portion of the CG pulse that occurs during the dead time would be lost. Second, the PDD was designed to turn off during high rates of successive triggers to conserve memory during episodes of glint off the spacecraft or bodies of water. Once a trigger count threshold was reached (often 10) over a short time interval (often 40 ms), the instrument would stop triggering until the next pulse-per-second signal. This prevented the PDD from resolving optical pulses that occurred late (hundreds of milliseconds) into long-lasting lightning flashes.

Third, the PDD could trigger on energetic particle impacts on the instrument, particularly over the South Atlantic Anomaly (SAA). Unlike the lightning imager on FORTE, the PDD had the ability to natively screen for these energetic particle impacts using an onboard filter. In its self-triggering mode, the PDD only generated events when the digitized signal exceeded the instrument threshold for a prescribed number of consecutive samples. The sample count threshold was commandable between 0 and 31, and usually set to 5 (corresponding to 75 μs). However, this filter was not uniformly applied throughout the FORTE mission. To mitigate residual contamination, we emulate the 5-sample threshold in post-processing to remove energetic particle spikes.

After filtering the PDD data, we identify the WWLLN strokes associated with PDD events. We first subset the daily catalog of WWLLN strokes to identify those that occur near the FORTE satellite subpoint around the time of the PDD event. Once we have the candidate list, we compute the Time Of Flight (TOF) of the corresponding optical signals from each WWLLN stroke to FORTE. Finally, we compare the TOF-corrected event times to the PDD event times. To account for potential physical and scattering delays in the optical signals (Suszcynsky et al., 2000; Peterson, 2022), we consider any event that occurs within the millisecond before the PDD trigger time to be a valid match. We only include PDD events matched with single WWLLN strokes in our analyses.

2.3 The Geostationary Lightning Mapper (GLM)

GLM is a pixelated lightning imager that records the scene below the GOES satellites in a narrow spectral band (777.4 nm) and triggers on transient increases in pixel energies during 2-

ms integration frames. Individual pixel detections are referred to as "events" in the GLM parlance, and they are clustered into larger-scale features that approximate lightning processes (Mach, 2020). Clusters of events in the same integration frame that form a contiguous region on the GLM imaging array are termed "groups" and approximate optical pulses. Groups that occur in close proximity in space and time are then clustered into features approximating lightning flashes using a Weighted Euclidian Distance (WED) model. GLM flashes and their constituent features are also used to generate meteorological imagery (Bruning et al., 2019) that provides additional context for GLM and WWLLN detections.

We do not use the operational GLM data products, however. These datasets provided by NOAA are degraded by hard limits coded into the GLM ground system software that split large or long-lasting flashes into pieces. Instead, we have created a repaired version of the GLM cluster feature data that mitigates these issues (Peterson, 2019). We also use this repaired dataset to construct meteorological GLM imagery. Our gridded products further differ from those in Bruning et al. (2019) because they are based on group-level rather than event-level data to reduce biases from radiative transfer effects across the cloud scene (Peterson et al,. 2017; Peterson, 2021a). We use GOES-16 data from 2018 to 2022 and GOES-17 data from 2019-2022 matched with WWLLN events in this study. However, our analysis of GLM superbolts focuses on observations from both satellites during the year 2020.

Due to a combination of GLM parallax (Virts and Koshak, 2020), WWLLN location uncertainties, and phenomenological differences, GLM often reports no lightning at the locations of WWLLN high energy events during the 15-minute data packet associated with the WWLLN stroke. Rather than match WWLLN strokes to GLM groups, we place our focus on linking these WWLLN events to their parent thunderstorm region. We accomplish this by identifying the nearby (i.e., within 0.25 degrees) gridpoint with the greatest value in the Flash Extent Density (FED: Lojou and Cummins, 2004) imagery product. FED is a spatial representation of GLM flash rates, and this peak value should correspond to the most active thunderstorm region in the vicinity of the WWLLN stroke.

3 Results

3.1 WWLLN Energies from FORTE PDD Events including Superbolts

The FORTE PDD is the best available analog for comparing the energies reported by WWLLN with optical outputs compatible with Turman (1977)'s study because it was a broadband sensor with a large dynamic range. GLM is not ideal because it measures narrowband energies integrated over milliseconds, while space-based photometers saturate before reaching the superbolt threshold.

The scatterplots in Figure 1 compare FORTE PDD peak optical powers (Figure 1a) and total optical energies (Figure 1b) with WWLLN energies during the last year of the PDD record. All single-matched WWLLN events are shown in light blue, while only cases that pass the filters used by Holzworth et al. (2019) are shown in dark blue. The PDD recorded 24 superbolts matched with WWLLN events during this period, including four 300 GW cases. The WWLLN

strokes in 8 superbolt events passed Holzworth et al. (2019)'s quality filters. Yet, the energies reported by WWLLN for these superbolts are quite low, ranging from 700 J to $2x10^4$ J – two orders of magnitude or more below the WWLLN high energy event threshold.

While there is a positive correlation between WWLLN VLF energies and both peak optical power and total optical energy that can be noted in Figure 1a and b, the upward slopes are insufficient to reach the WWLLN energy threshold within the range of optical events that have been recorded from lightning. Moreover, the top matched WWLLN events produce optical outputs well below expectations for a superbolt event.

The FORTE PDD data confirm that energetic WWLLN events are responding to a different set of physical mechanisms than optical superbolts, and we should not expect one to imply the other – even if they have a similar pattern of occurrence.

3.2 The Most Energetic WWLLN and GLM Lightning

We analyzed the top GLM superbolt cases in our quality-controlled database from the year 2020 and all quality-filtered WWLLN energetic events > 1 MJ from 2018 to 2022. We found that these two different types of energetic lightning occurred in conflicting meteorological contexts. The top GLM superbolt shown in Figure 2 is demonstrative of GLM superbolts. Figure 2a shows the structure of the flash (greyscale line segments), the location of the superbolt (yellow circle), and locations of WWLLN strokes in all ongoing flashes at the time of the superbolt (white stars) overlaid on top of GOES-16 Advanced Baseline Imager (ABI: Schmit et al., 2018) 10.3 μm infrared brightness temperature imagery. The domain of the plot is chosen to encompass the lightning-producing portion of the storm, which is depicted in the meteorological GLM imagery products shown in Figure 2 b-d. Flash Extent Density (FED) spatial flash rates are shown in Figure 2b. Mean flash extent (measured between the most distant points in each flash) is shown in Figure 2c. Mean flash duration is shown in Figure 2d. The ABI imagery is preserved, but changed to greyscale in these plots.

This 7.3 MJ GLM superbolt occurred midway through a long-horizontal GLM megaflash spanning 242 km between its most distant points. This flash produced 6 WWLLN strokes along its path beginning in the northeast and propagating south and west along multiple branches, as depicted in Figure 1a. The superbolt was located in a region of low flash rates (Figure 2b), large flash extents (Figure 2c), and long flash durations (Figure 2d) consistent with electrified stratiform clouds. By contrast, the active convective cells in the storm (to the north and west) produce frequent small / short-lived flashes.

The GLM light curve from this flash is shown in Figure 2e with the superbolt (yellow circle) and only the WWLLN strokes associated with the flash (white stars) overlaid. The GLM superbolt coincided with a WWLLN stroke, but the VLF energy from this extreme optical event was only ~10^4 J – two orders of magnitude below the WWLLN threshold. As we saw with the FORTE PDD, extreme optical emission does not correlate with exceptional VLF energies.

Instead, our survey of all quality controlled WWLLN high energy event cases during the public GLM data record reveals a different origin for these exceptional lightning discharges. The top case – a 6.7 MJ WWLLN stroke – is shown in Figure 3 and is representative of these events.

Instead of large megaflashes that are well-resolved by GLM, WWLLN high energy events occur in small convective flashes. Due to the small size of the flash in Figure 3, we replaced its horizontal structure (line segments in Figure 2) with black dots depicting the group centroid locations. We also included raw level-0 events (white dots), some of which are removed in level-2 filtering (grey dots).

The WWLLN high energy event occurred simultaneously with two additional WWLLN strokes located to the west and south in Figure 3a. As these additional strokes lacked energy measurements, we position them at 100 J in Figure 3e out of convenience. However, we speculate that they may be artifacts of the WWLLN geolocation algorithm caused by the high-energy event having a complex waveform shape. Interrogation of the station waveform data would be required to confirm, but this data is not preserved for longer than a few days (Holzworth et al., 2019).

Regardless, the WWLLN high energy event location in Figure 3 is co-located with the coldest cloud-tops in the thunderstorm, representing an intense updraft. Usually, strong convection generates frequent small discharges (Bruning and MacGorman, 2013) that are constantly neutralizing the charge separation generated by the updraft. In this WWLLN high energy event case, the flash sizes and durations are consistent with ordinary convection, but the FED values in Figure 3b are quite low.

The WWLLN high energy event occurred at the beginning of the GLM flash. The coherency filter in the GLM level-2 software rejects the first group in all flashes. These removed events are preserved at level-0 (white dots) and are no more energetic than the events later in the flash. This is consistent with other cases where the WWLLN high energy event is separated by up to hundreds of milliseconds from the nearest GLM activity and, when there is coincidence with GLM groups, their optical energies are modest at best. As with the FORTE PDD, none of the WWLLN high energy events that we examined are also GLM superbolts.

3.3 Meteorological Context of WWLLN High Energy Events and GLM Superbolts

To generalize the findings of our case analysis, we compiled statistics for the GLM gridded products associated with WWLLN high energy events and GLM superbolts using a 1 MJ threshold in either case. Statistics of the gridded products shown in Figures 2 and 3 are presented in Figure 4: Flash Extent Density (Figure 4a), mean flash extent (Figure 4b), and mean flash duration (Figure 4c). These histograms indicate that the cases in Figures 2 and 3 are representative of the broader trends. WWLLN high energy events originate in storm regions that have distinctly smaller and short-lived flashes compared to superbolts – consistent with convection – but also with low flash rates that are comparable to stratiform clouds. Animating the plots of WWLLN high energy events like Figure 3 (omitted for brevity) clarifies that the low flash rates in Figure 4a arise from storms that are either decaying (as in Figure 3) or starting to produce lightning (including after a pause in GLM / WWLLN detections).

While future work is required to identify the source of the intense VLF emissions, our initial analyses show that WWLLN high energy events could represent a unique class of convective discharge that would merit its own term. In the meantime, we speculate two possible origins for these events. First, they could be a kind of discharge that radiates strongly in the VLF

but not optical, like CIDs to VHF. Second, they could be related to the changing thunderstorm dynamics permitting more charge than usual to be amassed before the WWLLN stroke.

4 Conclusions

After comparing the VLF energies reported by WWLLN with measurements from two optical instruments – the PDD on the FORTE satellite, and GLM – we conclude that WWLLN high energy events are not optical superbolts. Optical superbolts are associated with long-horizontal lightning flashes in low flash rate regions outside of the convective core of the thunderstorm. The WWLLN energies from superbolts are not remarkable – 10^3 – 10^5 J, but notably less than the 10^6 J WWLLN high energy event threshold. By contrast, WWLLN high energy events occur within convective storm regions with low flash rates despite the otherwise typical prevalence of small, short-lived flashes and overshooting top signatures marking intense updrafts in the ABI infrared imagery.

Based on these observations, we hypothesize that the extreme VLF energies reported by WWLLN may arise in two ways. The first is a possible yet-to-be identified discharge that radiates strongly in the VLF but not optical. The second is the changing thunderstorm dynamics permitting an unusual amount of charge to be stored between convective flashes, which is then neutralized during the high energy WWLLN stroke. This could explain the prominence of high peak current negative polarity strokes in Holzworth et al. (2019), while the limited sizes of convective flashes explain the lack of intense optical output. We need additional measurements of thunderstorms producing WWLLN high energy events to determine whether this hypothesis is valid. In any case, WWLLN high energy events appear to correspond to a unique class of discharge distinct from optical superbolts.

Acknowledgments

Los Alamos National Laboratory is operated by Triad National Security, LLC, under contract number 89233218CNA000001.

Open Research

The FORTE PDD and GLM superbolt data used in this study are available at the Harvard Dataverse via DOI: 10.7910/DVN/RV39JT, (Peterson, 2020). Reprocessed GLM data are available from the NASA Global Hydrometeorology Resource Center DAAC at DOI:

10.5067/GLM/CIERRA/DATA101 (Peterson, 2021b). The University of Washington maintains a list of WWLLN high energy strokes at http://wwlln.net/publications/LargeStrokes.txt.

References

Abarca, S. F., Corbosiero, K. L., & Galarneau Jr, T. J. (2010). An evaluation of the worldwide lightning location network (WWLLN) using the national lightning detection network (NLDN) as ground truth. *Journal of Geophysical Research: Atmospheres*, *115*(D18).

Albrecht, R. I., Goodman, S. J., Buechler, D. E., Blakeslee, R. J., & Christian, H. J. (2016). Where are the lightning hotspots on Earth?. *Bulletin of the American Meteorological Society*, *97*(11), 2051-2068.

Bruning, E. C., & MacGorman, D. R. (2013). Theory and observations of controls on lightning flash size spectra. *Journal of the Atmospheric Sciences*, *70*(12), 4012-4029.

Bruning, E. C., Tillier, C. E., Edgington, S. F., Rudlosky, S. D., Zajic, J., Gravelle, C., ... & Meyer, T. C. (2019). Meteorological imagery for the geostationary lightning mapper. *Journal of Geophysical Research: Atmospheres*, *124*(24), 14285-14309.

Christian, H. J., Blakeslee, R. J., Boccippio, D. J., Boeck, W. L., Buechler, D. E., Driscoll, K. T., ... & Stewart, M. F. (2003). Global frequency and distribution of lightning as observed from space by the Optical Transient Detector. *Journal of Geophysical Research: Atmospheres*, *108*(D1), ACL-4.

Cummins, K. L., & Murphy, M. J. (2009). An overview of lightning locating systems: History, techniques, and data uses, with an in-depth look at the US NLDN. *IEEE transactions on electromagnetic compatibility*, *51*(3), 499-518.

Dowden, R. L., Brundell, J. B., & Rodger, C. J. (2002). VLF lightning location by time of group arrival (TOGA) at multiple sites. *Journal of Atmospheric and Solar-Terrestrial Physics*, *64*(7), 817-830.

Holzworth, R. H., McCarthy, M. P., Brundell, J. B., Jacobson, A. R., & Rodger, C. J. (2019). Global distribution of superbolts. *Journal of Geophysical Research: Atmospheres*, *124*(17-18), 9996-10005.

Kirkland, M. W., Suszcynsky, D. M., Guillen, J. L. L., & Green, J. L. (2001). Optical observations of terrestrial lightning by the FORTE satellite photodiode detector. *Journal of Geophysical Research: Atmospheres*, *106*(D24), 33499-33509.

Light, T. E. L. (2020). A retrospective of findings from the FORTE satellite mission. *Journal of Geophysical Research: Atmospheres*, *125*(9), e2019JD032264.

Light, T. E. L., & Jacobson, A. R. (2002). Characteristics of impulsive VHF lightning signals observed by the FORTE satellite. *Journal of Geophysical Research: Atmospheres*, *107*(D24), ACL-8.

Lojou, J.-Y., & Cummins, K. L. (2004). On the representation of two- and three-dimensional total lightning information. In Preprints, Conference on Meteorological Applications of Lightning Data, Paper 2.4, AMS Annual Meeting, San Diego, CA, USA.

Mach, D. M. (2020). Geostationary Lightning Mapper clustering algorithm stability. *Journal of Geophysical Research: Atmospheres*, *125*(5), e2019JD031900.

Peterson, M. (2019). Research applications for the Geostationary Lightning Mapper operational lightning flash data product. *Journal of Geophysical Research: Atmospheres*, *124*(17-18), 10205-10231.

Peterson, M. (2020). Lightning Superbolt Data, https://doi.org/10.7910/DVN/RV39JT, Harvard Dataverse, V2.

Peterson, M. (2021a). Holes in optical lightning flashes: Identifying poorly transmissive clouds in lightning imager data. *Earth and Space Science*, *8*(2), e2020EA001294.

Peterson, M. (2021b). GLM-CIERRA. https://doi.org/10.5067/GLM/CIERRA/DATA101

Peterson, M. (2022). FORTE measurements of global optical lightning waveforms and implications for optical lightning detection. *Earth and Space Science*, *9*(6), e2022EA002280.

Peterson, M., & Liu, C. (2011). Global statistics of lightning in anvil and stratiform regions over the tropics and subtropics observed by the Tropical Rainfall Measuring Mission. *Journal of Geophysical Research: Atmospheres*, *116*(D23).

Peterson, M., Rudlosky, S., & Deierling, W. (2017). The evolution and structure of extreme optical lightning flashes. *Journal of Geophysical Research: Atmospheres*, *122*(24), 13-370.

Peterson, M., & Kirkland, M. W. (2020). Revisiting the detection of optical lightning superbolts. *Journal of Geophysical Research: Atmospheres*, *125*(23), e2020JD033377.

Peterson, M., & Lay, E. (2020). GLM observations of the brightest lightning in the Americas. *Journal of Geophysical Research: Atmospheres*, *125*(23), e2020JD033378.

Peterson, M., Mach, D., & Buechler, D. (2021). A global LIS/OTD climatology of lightning flash extent density. *Journal of Geophysical Research: Atmospheres*, *126*(8), e2020JD033885.

Rudlosky, S. D., Goodman, S. J., Virts, K. S., & Bruning, E. C. (2019). Initial geostationary lightning mapper observations. *Geophysical Research Letters*, *46*(2), 1097-1104.

Schmit, T. J., Lindstrom, S. S., Gerth, J. J., & Gunshor, M. M. (2018). Applications of the 16 spectral bands on the Advanced Baseline Imager (ABI).

Suszcynsky, D. M., Kirkland, M. W., Jacobson, A. R., Franz, R. C., Knox, S. O., Guillen, J. L. L., & Green, J. L. (2000). FORTE observations of simultaneous VHF and optical emissions from lightning: Basic phenomenology. *Journal of Geophysical Research: Atmospheres*, *105*(D2), 2191-2201.

Thomas, R. J., Krehbiel, P. R., Rison, W., Hamlin, T., Boccippio, D. J., Goodman, S. J., & Christian, H. J. (2000). Comparison of ground-based 3-dimensional lightning mapping observations with satellite-based LIS observations in Oklahoma. *Geophysical research letters*, *27*(12), 1703-1706.

Thomson, N. R. (2010). Daytime tropical D region parameters from short path VLF phase and amplitude. *Journal of Geophysical Research: Space Physics*, *115*(A9).

Turman, B. N. (1977). Detection of lightning superbolts. *Journal of Geophysical Research*, *82*(18), 2566-2568.

Virts, K. S., & Koshak, W. J. (2020). Mitigation of geostationary lightning mapper geolocation errors. *Journal of Atmospheric and Oceanic Technology*, *37*(9), 1725-1736.

Whipple, F. J. W. and Scrase, F. J. (1936). Point-discharge in the electric field of the Earth. *Geophys. Mem. VII*, *68*, 1-20.

Williams, E. R. (2005). Lightning and climate: A review. *Atmospheric research*, *76*(1-4), 272-287.

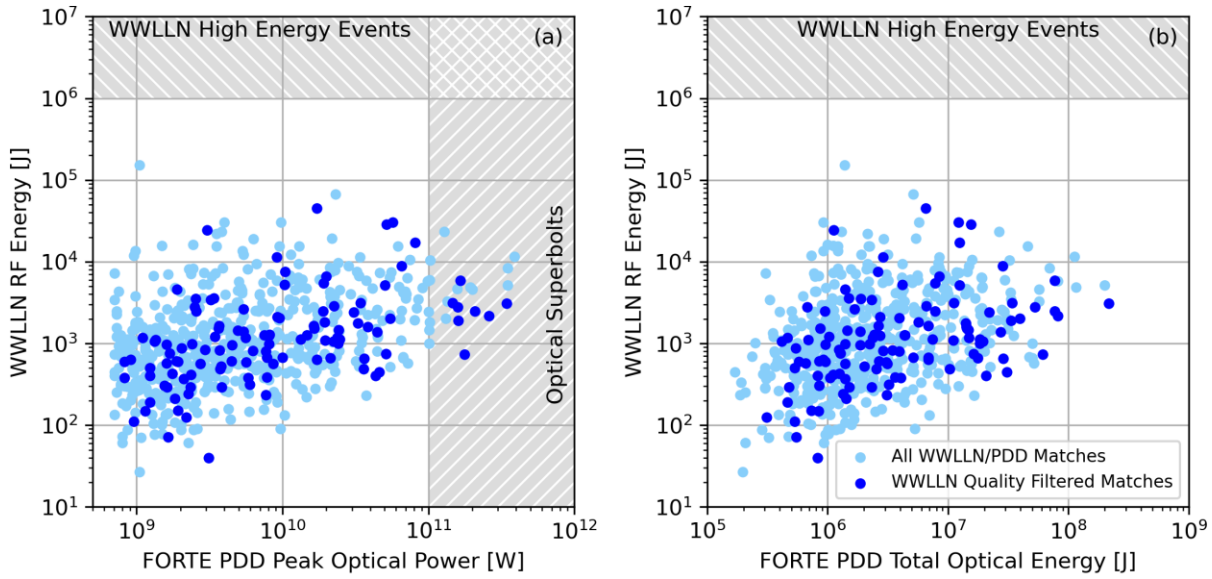

Figure 1. Two-dimensional histograms of the (a) peak optical power and (b) total optical energy of PDD events matched to single WWLLN strokes and WWLLN VLF source energies. PDD measurements have been normalized to the source, as in Turman (1977). All WWLLN strokes are shown in light blue, while strokes meeting the filters used in Holzworth et al. (2019) are shown in dark blue.

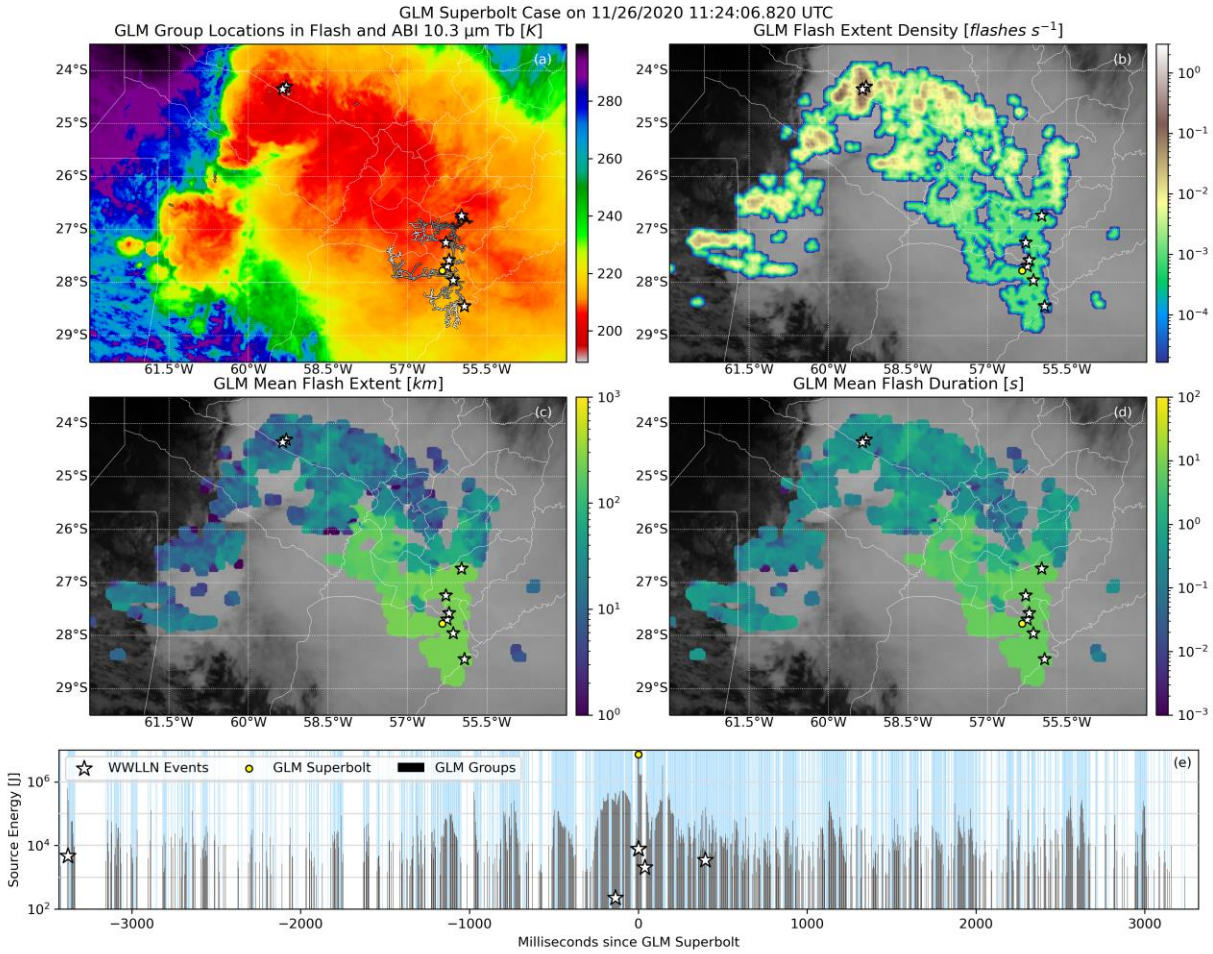

433

434 **Figure 2**. GOES-16 observations of the top GLM superbolt case during the year 2020. GLM (a)
435 group-derived flash structure (greyscale lines representing time, with darker signifying older),
436 (b) Flash Extent Density, (c) mean flash extent, and (d) mean flash duration are overlaid on top
437 of ABI 10.3 μm infrared imagery (color contours in a, greyscale in b-d). WWLLN strokes
438 around the time of the superbolt are overlaid with star symbols. The superbolt location is
439 indicated with a yellow circle. (e) GLM light curve for the superbolt-producing flash. Groups
440 (grey) are plotted according to their optical energies on top of a blue background highlighting the
441 frame. WWLLN strokes (stars) in the flash are plotted according to their VLF energies.

442

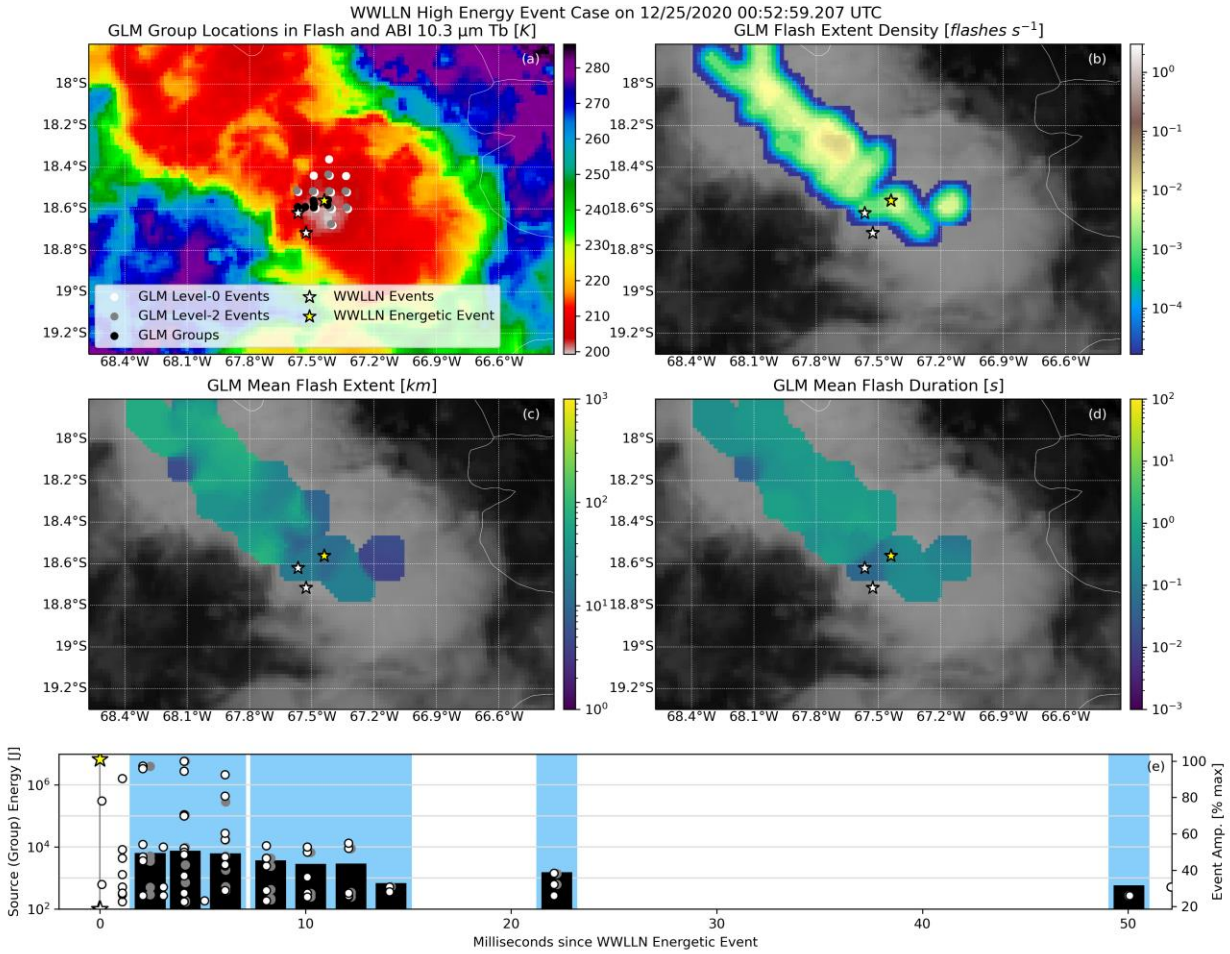

Figure 3. As in Figure 1, but showing the top WWLLN high energy event during the GLM public data record. The WWLLN high energy event is colored yellow. GLM raw level-0 (white circles) and filtered level-2 (grey circles) events are also overlaid in (a) and (e).

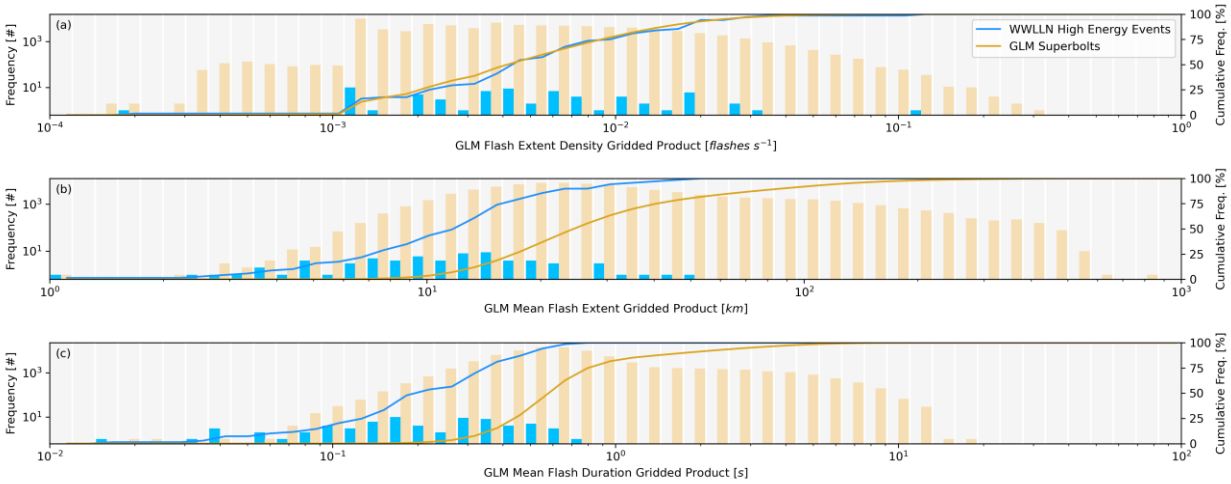

Figure 4. Histograms of the GLM (a) Flash Extent Density, (b) mean flash extent, and (c) mean flash duration gridded products corresponding to GLM superbolts (blue) and WWLLN high energy events (wheat).